COMPARISON OF M^3 (VNIR) AND DIVINER (MIR) DATA OF OLIVINE-BEARING REGIONS OF THE MOON. J. A. Arnold[1], T. D. Glotch[1], P. G. Lucey[2] and E. Song[2] [1]Stony Brook University (255 Earth and Space Sciences, Stony Brook University, Stony Brook NY, 11794-2100; Jessica.a.arnold@stonybrook.edu) for first author, [2] Hawaii Institute of Geophysics and Planetology, University of Hawaii.

Introduction: Locations on the Moon with olivine-bearing lithologies have been detected by visible near-IR (VNIR) instruments such as the Chandrayaan-1 Moon Mineralogy Mapper (M^3) [1,2] and Kaguya Spectral Profiler (SP) [3]. Prior to this, olivine-rich exposures had been detected in a handful of areas including the central peak of Copernicus and ejecta of Aristarchus crater with both telescopic data [4,5] and the Clementine UVVIS camera [6].

It is difficult to estimate olivine abundance by using either VNIR or mid-IR data alone. Plagioclase feldspar has a weak feature at 1.25 µm due to minor Fe^{2+} incorporated into the crystal structure. This absorption will be obscured in the presence of olivine or pyroxene, making it difficult to constrain abundances from nonlinear mixture modeling of near-IR data [7]. In the mid-IR, pure or nearly pure olivine would be distinguishable with Diviner Lunar Radiometer Experiment data by the concavity of Channels 3-5 and elevated CF position (>8.5 µm) [8]. However, a mixture of olivine and plagioclase would have intermediate values similar to pyroxene. For areas that do not have the characteristic 2 µm pyroxene Fe^{2+} absorption in the VNIR, we can use mid-IR data to estimate the percentages of plagioclase and olivine assuming a two-component system.

Datasets and Methods: This study uses data from M^3 to confirm the location of olivine-bearing regions detected by Kaguya's SP. For each area of interest, index maps of the 1- and 2-µm integrated band depths were generated from the relevant M^3 reflectance data strip. Band depths are calculated by summing the difference between the actual reflectance and the continuum as fit by a line over the absorption band. We used the accompanying M^3 location files to find the coordinates of spots with a high 1-µm band depth index, but low 2-µm band depth index and a large enough spatial extent to be visible at Diviner's spatial resolution.

For each of these locations, we looked at mid-IR emissivity derived from Diviner radiance data. Diviner has three "8µm" channels located at 7.80 µm (Ch 3), 8.25 µm (Ch 4), and 8.55 µm (Ch 5), chosen to distinguish the Christiansen (CF), which can be used to characterize the silicate mineralogy of the lunar surface [8]. Daytime data was constrained to less than 50° from the equator and a solar incidence angle correction as described in [9] was applied. We binned the data at either 128 or 256 pixels per degree for regional analysis. Emissivity data was obtained by dividing the measured radiance of each channel by the black body radiance of the maximum brightness temperature of all the channels for each pixel.

Diviner emissivity and M^3 reflectance spectra were extracted from and averaged over polygons covering nearly identical spots on the lunar surface (see Figure 1). We used visible color images from the Lunar Reconnaissance Orbiter Camera (LROC) Wide Angle Camera (WAC) to verify the location and make small adjustments to the area of Diviner data extraction when necessary.

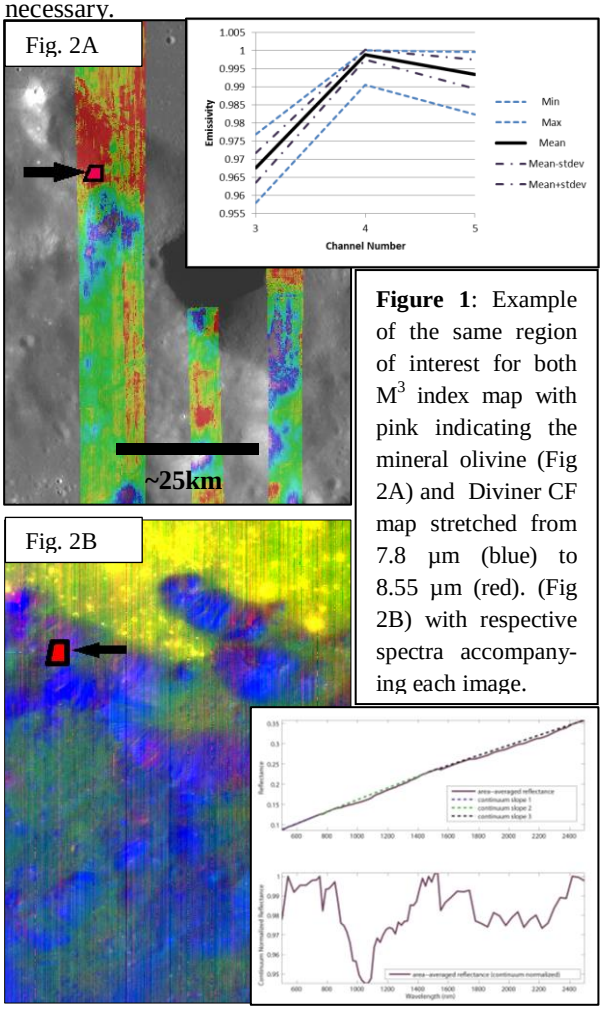

Figure 1: Example of the same region of interest for both M^3 index map with pink indicating the mineral olivine (Fig 2A) and Diviner CF map stretched from 7.8 µm (blue) to 8.55 µm (red). (Fig 2B) with respective spectra accompanying each image.

Lunar Environment Spectra: We compare Diviner-derived emissivity to laboratory emissivity spectra of fine-grained (<63 µm) two-component powder mixtures of anorthite and forsterite acquired in a simulated lunar environment (SLE). The relative weight

percentages of the components were varied, to measure changes in the Christiansen feature (CF) position with mixture composition. These samples are described in [10]. Emission spectra were measured in a chamber that approximates the thermal environment of the lunar surface created by vacuum conditions [11].

Although a mixture does not necessarily have one CF, but a feature that is an average of each mineral's CF, the lab spectra were convolved to the Diviner filter functions and a 'Diviner CF position' was calculated. The 'Diviner CF position' vs. weight percent was fit with a spline. This empirical curve was then applied to the averaged Diviner CF for the olivine-rich regions of interest to give a rough estimate of forsterite/anorthite ratios for these areas.

Discussion and Results: The longer-wavelength CF position of Fe-rich olivine and unique spectral shape would lower the threshold for olivine detectability by Diviner. Lack of data for a variety of olivine compositions along with the non-linearity of mixing makes it difficult to calculate exact abundances from the spectral shape of Ch 3-5 alone, so these olivine abundance estimates represent a maximum possible amount present. Additionally, the CF position is affected by space weathering, shifting to longer wavelengths on more optically mature surfaces of a given composition [12]. The areas we have studied have a wide range of calculated olivine abundances, ranging from ~60% up through >90% (Figure 2). One area has an estimated olivine percentage of >100% based on SLE forsterite data. Based on end-members derived from factor analysis and target transformation (FATT) [12] of M^3 data, this area may contain Fe-rich olivine (Figure 3). We also applied this technique to other areas to show that most exposures have low Fe-content (high Fo #).

References: [1] Peiters C. M. et al. (2009) *Curr. Sci*, *96*, 500-505. [2] Mustard J.F. et al. (2011) *JGR*, 116. [3] Yamamoto S. et al. (2010) *Nat. Geosci.*, *3*, 8, 533- 536. [4] Pieters C. M. (1982) *Science*, *215*, 59-61. [5] Lucey P. G. et al. (1986) *J. Geophys. Res. 91*, D344-D354. [6] Tompkins S. and Pieters, C. M. (1999) *Meteorit. & Planet. Sci. 34*, 25-41. [7] Issacson P. J. et al. (2011) *Meteorit. & Planet. Sci., 46*, 228-251. [8] Greenhagen B.T. et al. (2010) *Science*, *329*, 1507-1509. [9] Greenhagen B.T. et al. (2011) *LPS XLIII*, Abstract #2679. [10] Arnold J. A. et al. (2013) *LPS XLIV*, Abstract #2972. [11] Thomas I. R. et al. (2012) *Rev. Sci. Instrum. 83*, 124502. [12] Glotch T. D. and Bandfield J. L. (2006) *J. Geophys. Res., 111*, E12S06. [12] Lucey P. G. et al. (2010) LPS XLI, Abstract #1600.

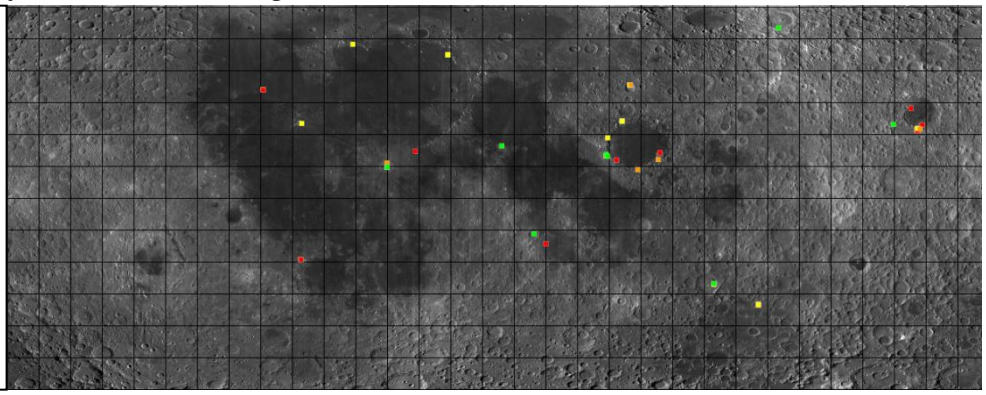

Figure 2: Global map of olivine-rich locations on the Moon with colors indicating a rough abundance estimate.
Blue=~50-60%
Green=~60-70%
Yellow=~70-80%
Orange=~80-90%
Red=~90-100%

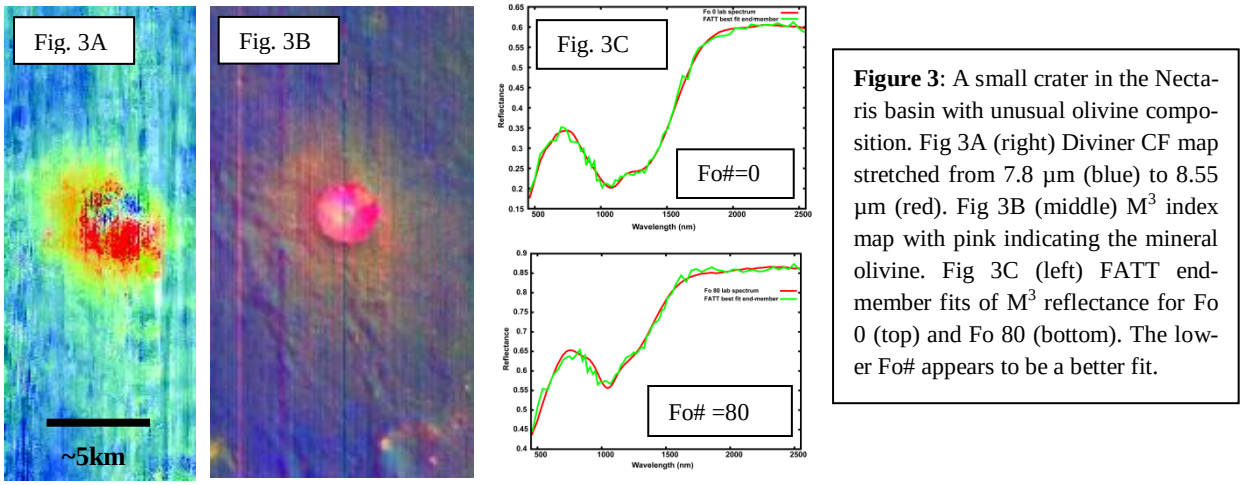

Figure 3: A small crater in the Nectaris basin with unusual olivine composition. Fig 3A (right) Diviner CF map stretched from 7.8 µm (blue) to 8.55 µm (red). Fig 3B (middle) M^3 index map with pink indicating the mineral olivine. Fig 3C (left) FATT end-member fits of M^3 reflectance for Fo 0 (top) and Fo 80 (bottom). The lower Fo# appears to be a better fit.